ATTACHMENT 15

Westinghouse Letter LTR-SGMP-09-109 NP-Attachment, "Response to NRC Request for Additional Information on H*; RAI #4; Model F and Model D5 Steam Generators" (Non-Proprietary)

Westinghouse Electric Company

Response to NRC Request for Additional Information on H*; RAI #4; Model F and Model D5 Steam Generators

August 25, 2009

Westinghouse Electric Company LLC
P.O. Box 158
Madison, PA 15663

*Electronically approved records are authenticated in the Electronic Document Management System

Response to
NRC Request for Additional Information on H*; RAI #4;
Model F and Model D5 Steam Generators

References:

1. NL-09-0547, Vogtle Electric Generating Plant License Amendment Request to Revise Technical Specification(TS) Sections 5.5.9, "Steam Generator (SG) Program" and TS 5.6.10, "Steam Generator Tube Inspection Report for Permanent Alternate Repair Criteria," Southern Company, May 19, 2009.

2. RS-09-071, "License Amendment Request to Revise Technical Specifications (TS) for Permanent Alternate Repair Criteria," Exelon Nuclear, June 24, 2009.

3. CP-200900748, Log # TXX-09075, "Comanche Peak Steam Electric Station (CPSES) Docket Nos. 50-445 and 50-446, License Amendment Request 09-007, Model D5 Steam Generator Alternate Repair Criteria," Luminant, June 8, 2009.

4. SBK-L-09118, "Seabrook Station: License Amendment Request 09-03; Revision to Technical Specification 6.7.6.k, "Steam Generator (SG) Program," for Permanent Alternate Repair Criteria (H*)," May 28, 2009.

5. Vogtle Electric Generating Plant, Units 1 and 2, Request for Additional Information Regarding Steam Generator Program (TAC Nos. ME1339 and ME1340)," United States Nuclear Regulatory Commission, July 10, 2009.

6. Braidwood Station, Units 1 and 2, and Byron Station, Unit Nos. 1 and 2 – Request for Additional Information Related to Steam Generator Permanent Alternate Repair Criteria (TAC Nos. ME1613, ME1614, ME1615, and ME1616)," United States Nuclear Regulatory Commission, July 20, 2009.

7. Comanche Peak Steam Electric Station, Units 1 and 2 – Request for Additional Information Regarding the Permanent Alternate Repair Criteria License Amendment Request (TAC Nos. ME1446 and ME1447)," United States Nuclear Regulatory Commission, July 23, 2009.

8. WCAP-17071-P, "H*: Alternate Repair Criteria for the Tubesheet Expansion Region in Steam Generators with Hydraulically Expanded Tubes (Model F)," Westinghouse Electric LLC, April 2009.

9. WCAP-17072-P, "H*: Alternate Repair Criteria for the Tubesheet Expansion Region in Steam Generators with Hydraulically Expanded Tubes (Model D5)," Westinghouse Electric LLC, May 2009.

10. "Vogtle Electric Generating Plant, Units 1 and 2, Request for Additional Information Regarding Steam Generator Program (TAC Nos. ME1339 and ME1340)," United States Nuclear Regulatory Commission, August 5, 2009

11. LTR-SGMP-09-100, "Response to NRC Request for Additional Information on H*; Model F and Model D5 Steam Generators," August 2009

12. LTR-NRC-09-26, "LTR-SGMP-09-66 P-Attachment, "White Paper: Low Temperature Steam Line Break Contact Pressure and Local Tube Bore Deformation Analysis for H* (Proprietary)," Westinghouse Electric Company LLC, May 13, 2009.

13. Seabrook Station, Unit No. 1- Request for Additional Information Regarding Steam Generator Program (TAC Nos. ME1386)," United States Nuclear Regulatory Commission, August 13, 2009

Introduction

In response to formal requests for technical specification amendments, References 1, 2, 3 and 4, the USNRC formally requested additional information in References 5, 6, 7 and 13. The Vogtle, Seabrook, Byron/Braidwood and Comanche Peak requests for a permanent license amendment to implement H* represent the Model F and Model D5 steam generators for which the H* technical justification is provided in References 8 and 9.

Subsequent to the initial issue of the RAI (References 5, 6, 7 and 13), the NRC issued follow-up questions (Reference 10) to questions numbers 4, 20 and 24 and an additional request regarding a technical specification (TS) commitment for applying the leakage factors. Except for RAI#4, responses to all of the RAIs, including the follow-up questions in Reference 10, were provided in Reference 11. The affected licensees provided separate responses in regard to the commitment for applying leakage factors.

The response to RAI#4 required additional explanation as discussed with the NRC staff on August 11, 2009 and was, therefore, not included in Reference 11. The additional questions related to RAI#4 that were identified during the August 11, 2009 telephone conference were summarized by Westinghouse and were the basis of the discussion at a meeting among the NRC, several licensees and Westinghouse on August 17 and 18, 2009. These additional questions are reproduced in the response to RAI#4, below. Specific discussion is included in the response to address the additional questions.

To summarize, this document provides the response to the initial RAI#4 as included in References 5, 6, 7 and 13, response to the follow-up question relating to RAI#4 in Reference 10 and response to the additional questions raised during the conference call on August 11, 2009.

Utilities, other than referenced in this document, have requested amendments to their licensees in parallel with the response to these RAI's. The technical RAIs are generic in nature because the analysis methods are the same for all affected plants. Therefore, this response to RAI#4 is generic for all Models of SGs that are candidates for application of H*. However, this letter

specifically augments Reference 11 to complete the responses to NRC RAIs for WCAP-17071-P (Model F H*) and WCAP-17072-P (Model D5 H*).

RAI Part A	*Vogtle*	*4. Reference 1, page 6-69: In Section 6.2.5.3, it is concluded that the tube outside diameter and the tubesheet tube bore inside diameter always maintain contact in the predicted range of tubesheet displacements. However, for tubes with through-wall cracks at the H* distance, there may be little or no net pressure acting on the tube for some distance above H*. In Tables 6-18 and 6-19, the fourth increment in the step that occurs two steps prior to the last step suggests that there may be no contact between the tube and tubesheet, over a portion of the circumference, for a distance above H*. Is the conclusion in Section 6.2.5.3 valid for the entire H* distance, given the possibility that the tubes may contain through-wall cracks at that location?*
	WCGS	*4. Reference 1, page 6-69: In Section 6.2.5.3, it is concluded that the tube outside diameter and the tubesheet tube bore inside diameter always maintain contact in the predicted range of tubesheet displacements. However, for tubes with through-wall cracks at the H* distance, there may be little or no net pressure acting on the tube for some distance above H*. In Tables 6-18 and 6-19, the fourth increment in the step that occurs two steps prior to the last step suggests that there may be no contact between the tube and tubesheet, over a portion of the circumference, for a distance above H*. Is the conclusion in 6.2.5.3 valid for the entire H* distance, given the possibility that the tubes may contain through-wall cracks at that location?*
	B/B	*4. Reference 1, Page 6-7: In Section 6.2.5.3, it is concluded that the tube outside diameter and the tubesheet tube bore inside diameter always maintain contact in the predicted range of tubesheet displacements. However, for tubes with through-wall cracks at the H* distance, there may be little or no net pressure acting on the tube for some distance above H*. In Tables 6-18 and 6-19, the fourth increment in the step that occurs two steps prior to the last step suggests that there may be no contact between the tube and tubesheet, over a portion of the circumference, for a distance above H*. Is the conclusion in 6.2.5.3 valid for the entire H* distance, given the possibility that the tubes may contain through-wall cracks at that location.*

	CPSES	*4. Reference 1, page 6-70: In Section 6.2.5.3, it is concluded that the tube outside diameter and the tubesheet tube bore inside diameter always maintain contact in the predicted range of tubesheet displacements. However, for tubes with through-wall cracks at the H* distance, there may be little or no net pressure acting on the tube for some distance above H*. In Tables 6-18 and 6-19, the fourth increment in the step that occurs two steps prior to the last step suggests that there may be no contact between the tube and tubesheet, over a portion of the circumference, for a distance above H*. Is the conclusion in Section 6.2.5.3 valid for the entire H* distance, given the possibility that the tubes may contain through-wall cracks at that location?*
	Seabrook	*4. Reference 1, page 6-69: In Section 6.2.5.3, it is concluded that the tube outside diameter and the tubesheet tube bore inside diameter always maintain contact in the predicted range of tubesheet displacements. However, for tubes with through-wall cracks at the H* distance, there may be little or no net pressure acting on the tube for some distance above H*. In Tables 6-18 and 6-19, the fourth increment in the step that occurs two steps prior to the last step suggests that there may be no contact between the tube and tubesheet, over a portion of the circumference, for a distance above H*. Is the conclusion in 6.2.5.3 valid for the entire H* distance, given the possibility that the tubes may contain through-wall cracks at that location?*

Part B: The additional questions relating to RAI#4 as provided in Reference 10 are:

Address following questions as part of response to RAI#4 (Vogtle):

a. *Clarify the nature of the finite element model ("slice" model versus axisymmetric SG assembly model) used to generate the specific information in Tables 6-1, 2, and 3 (and accompanying graph entitled "Elliptical Hole Factors") of Reference 6-15. What loads were applied? How was the eccentricity produced in the model? (By modeling the eccentricity as part of the geometry? By applying an axisymmetric pressure the inside of the bore?) Explain why this model is not scalable to lower temperatures.*

b. *Provide table showing maximum delta diameters (total diameter distortion) and maximum eccentricities (maximum diameter minus minimum diameter) from the 3 dimensional (3-D) finite element analysis for normal operating and steam line break (SLB), for model F and D5.*

c. *In Figure 2 of the White Paper, add plot for original relationship between reductions in contact pressure and eccentricity as given in Reference 6-15 in the graph accompanying Table 6-3. Explain why this original relationship remains conservative*

in light of the new relationship. Explain the reasons for the differences between the curves.

d. *When establishing whether contact pressure increases when going from normal operating to steam line break conditions, how can a valid and conservative comparison be made if the normal operating case is based on the original delta contact pressure versus eccentricity curve and the SLB case is based on the new curve?*

Part C: Additional Questions Provided in the August 11, 2009 telephone conference:

a. Overall High Level Question

1. *Discuss if the eccentricity effect on contact pressure is occurring as described. It is the opinion of the NRC staff that the eccentricity effect may not be as significant as being reported by Westinghouse.*

b. Other Key Questions

1. *The eccentricities included in Table RAI 4-4 appear larger than anticipated. Need to confirm that positive contact pressure exists around the entire circumference of the tube and state this clearly in the response.*
2. *The difference between initial and final eccentricity included in Table RAI4-2 needs to be explained. In particular, the exclusive use of the relationship between initial eccentricity and scale factor in calculating contact pressure needs to be justified.*
3. *The basis for applying the correlation for scale factor outside an "eccentricity" range of between 1E-3 to 1E-4 inch in the calculation of contact pressure needs to be further explained. Values for displacements included in Table 6-18 (of WCAP-17071) suggest that contact pressure may be lost at displacement ranging between 1E-3 in to 1E-4 inch.*
4. *Provide the calculation basis for the upper and lower curves provided in Figure RAI 4-2*
5. *Resolve the apparent inconsistency between Item 4 on page 25 and the statement below Figure RAI4-1 regarding how the model in Figure RAI4-1 is loaded.*

c. Key Remaining Issues

1. *Provide the basis for why the ΔD_{hole} adjustment for contact pressure made using the old model remains conservative.*
2. *Provide an appropriate basis for demonstrating that joints tighten during a postulated SLB event. Why is it acceptable to compare the contact pressures calculated using the original model for NOP to the contact pressures calculated using the new model for SLB for the Model D5 SGs?*
3. *If both old and new models are conservative, is there an appropriate basis to show the relative conservatism of the methods?*

To facilitate a continuous response to the total RAI#4 questions, the questions received originally (Part A), those received as follow-up questions (Part B) and those identified during the 8/11/09 telephone conference (Part C) are re-arranged as noted below. The location of responses to specific questions is shown in bold type after the question. Also, in the responses, the specific questions addressed by the responses are repeated in bold type in the box at the start of the response.

Part C: Sub a.

Discuss if the eccentricity effect on contact pressure is occurring as described. It is the opinion of the NRC staff that the eccentricity effect may not be as significant as being reported by Westinghouse. ***(See Section 1.0)***

Part B

Address following questions as part of response to RAI#4 (Vogtle):

a. Clarify the nature of the finite element model ("slice" model versus axisymmetric SG assembly model) used to generate the specific information in Tables 6-1, 2, and 3 (and accompanying graph entitled "Elliptical Hole Factors") of Reference 6-15. What loads were applied? How was the eccentricity produced in the model? (By modeling the eccentricity as part of the geometry? By applying an axisymmetric pressure the inside of the bore?) Explain why this model is not scalable to lower temperatures. ***(See Section 1.2)***

b. Provide table showing maximum delta diameters (total diameter distortion) and maximum eccentricities (maximum diameter minus minimum diameter) from the 3 dimensional (3-D) finite element analysis for normal operating and steam line break (SLB), for model F and D5. ***(See Section 1.1)***

c. In Figure 2 of the White Paper, add plot for original relationship between reductions in contact pressure and eccentricity as given in Reference 6-15 in the graph accompanying Table 6-3. Explain why this original relationship remains conservative in light of the new relationship. Explain the reasons for the differences between the curves. ***(See Section 4.1)***

d. When establishing whether contact pressure increases when going from normal operating to steam line break conditions, how can a valid and conservative comparison be made if the normal operating case is based on the original delta contact pressure versus eccentricity curve and the SLB case is based on the new curve? ***(See Section 4.2)***

Part C: Sub b. Other Key Questions

1. *The eccentricities included in Table RAI 4-4 appear larger than anticipated. Need to confirm that positive contact pressure exists around the entire circumference of the tube and state this clearly in the response.* ***(See Section 3)***

2. *The difference between initial and final eccentricity included in Table RAI4-2 needs to be explained. In particular, the exclusive use of the relationship between initial eccentricity and scale factor in calculating contact pressure needs to be justified.* ***(See Section 1.2)***

3. *The basis for applying the correlation for scale factor outside an "eccentricity" range of between 1E-3 to 1E-4 inch in the calculation of contact pressure needs to be further explained. Values for displacements included in Table 6-18 (of WCAP-17071) suggest that contact pressure may be lost at displacement ranging between 1E-3 in to 1E-4 inch.* ***(See Section 2.0)***

4. *Provide the calculation basis for the upper and lower curves provided in Figure RAI 4-2.* ***(See Section 2.1)***

5. *Resolve the apparent inconsistency between Item 4 on page 25 and the statement below Figure RAI4-1 regarding how the model in Figure RAI4-1 is loaded.* ***(See Section 1.2)***

Part C: Sub c. Key Remaining Issues

1. *Provide the basis for why the ΔD_{hole} adjustment for contact pressure made using the old model remains conservative.* ***(See Section 2.2)***

2. *Provide an appropriate basis for demonstrating that joints tighten during a postulated SLB event. Why is it acceptable to compare the contact pressures calculated using the original model for NOP to the contact pressures calculated using the new model for SLB for the Model D5 SGs?* ***(See Section 2.3)***

3. *If both old and new models are conservative, is there an appropriate basis to show the relative conservatism of the methods?* ***(See Section 2.4)***

Part A: (Original RAI#4 from Reference 5)

Reference 1, Page 6-69: In Section 6.2.5.3, it is concluded that the tube outside diameter and the tubesheet tube bore inside diameter always maintain contact in the predicted range of tubesheet displacements. However, for tubes with through-wall cracks at the H distance, there may be little or no net pressure acting on the tube for some distance above H*. In Tables 6-18 and 6-19, the fourth increment in the step that occurs two steps prior to the last step suggests that there may be no contact between the tube and tubesheet, over a portion of the circumference, for a distance above H*. Is the conclusion in 6.2.5.3 valid for the entire H* distance, given the possibility that the tubes may contain through-wall cracks at that location?* ***(See Section 5.0)***

1.0 General Background on Approach and Models

Discuss if the eccentricity effect on contact pressure is occurring as described. It is the opinion of the NRC staff that the eccentricity effect may not be as significant as being reported by Westinghouse.

Response:

The reference structural model for the H* calculation as described in References 8 and 9 is a 3D FEA model that utilizes the equivalent properties approach for perforated plates in accordance with Reference 6-15 of the H* WCAP reports. This model provides the tubesheet displacements that are utilized in the calculation of H*. Included in the displacement output from the 3D FEA model are the radius and depth dependent x- and y- axis displacements for the tubesheet. These displacements are the input to the H* integrator model that uses the inputs to calculate contact pressures based on thick-shell equations. The tubesheet displacements from the FEA model indicate that the tubesheet bores become eccentric after application of all thermal and pressure loads. The displacement results from the 3D FEA model are the difference between the completely unloaded case and the fully loaded case for the conditions of interest (i.e., NOP, SLB).

The information from the 3D FEA model, that the tubesheet bores become eccentric, led to a question regarding continued tube-to-tubesheet contact in the eccentric tubesheet bore. The impact of tubesheet bore hole out-of-roundness (eccentricity) on the calculation of tube to-tubesheet contact pressures was originally addressed using a scale factor approach as described below and in Reference 6-15 of the H* WCAP reports. The fit developed in Reference 6-15 , a third order polynomial, was appropriate for the conditions for which it was developed but it provided physically impossible results when extrapolated significantly outside its data basis such as was the case for the SLB conditions for the Model D5 SGs.

To resolve this issue, a separate model, was developed as described in Section 6.2.5 and shown in Figure 6-48 of Reference 8 and 9, to assess tube-to-tubesheet contact under the fully loaded condition (e.g., ΔP and thermal loading) for the small eccentricities that were calculated during the much "colder" temperature postulated SLB conditions for the Model D5 SGs than for the Model F SGs. To properly represent the tube in tubesheet condition, this model considered a tubesheet equivalent cell (the local TS material around a tubesheet bore) and a tube. To address the question if continued contact would exist between the tube and tubesheet after the tubesheet bore becomes eccentric, the tube expansion was analytically simulated to provide a condition of tube to tubesheet contact in a non-eccentric tubesheet bore. This condition was the reference condition for the subsequent loading of the model by pressure loads (thermal loads were not included) and by applying displacement boundary conditions (e-bar) to simulate the expected range of tubesheet bore eccentricity. The unloaded, post-tube expansion simulation conditions of the model was the reference condition for the displacements provided in Tables 6-18 and 6-19 of the H* reports, References 8 and 9.

While eccentricity was the specific focus of this study because of the question raised about continued tube to tubesheet contact in an eccentric condition, the analytical model naturally also provided information on tubesheet bore dilation, the diametral growth of the tubesheet bore represented by the average of the maximum and minimum diameters of the eccentric tubesheet bore. Examination of the results from this model, as is discussed further below, resulted in two significant conclusions:

1. For the tubesheet bore eccentricities and dilation due to the applied loading in the limiting plants in the models of SG considered, the tube remains in contact with the tubesheet bore.

2. While tubesheet bore eccentricity contributes to the reduction in contact pressure between the tube and the tubesheet, tubesheet bore dilation appears to be the principal cause of reduction of contact pressure between the tube and the tubesheet.

1.1 Discussion of 3D FEA Model for H* Analysis

Provide table showing maximum delta diameters (total diameter distortion) and maximum eccentricities (maximum diameter minus minimum diameter) from the 3 dimensional (3-D) finite element analysis for normal operating and steam line break (SLB), for model F and D5.

Response:

The 3D FEA Model and its application for determining the tubesheet displacements are extensively described in Section 6 of the H* WCAP reports (References 8 and 9). It is important to note that the 3D FEA model includes the entire tubesheet complex (i.e., tubesheet, stub barrel, channelhead and divider plate) but excludes the tubes. The model utilizes an equivalent material approach from Reference 6-5 in the WCAP reports to represent the deformation of the tubesheet under the applied loading conditions (NOP, SLB/FLB). Displacements in Cartesian coordinates are calculated for these conditions at any location on the tubesheet. The displacements calculated are the changes from an unstressed, room temperature condition after all thermal and pressure loads appropriate to the operating conditions are applied. Application of a uniform temperature increase causes uniform dilation at each tubesheet bore. Application of pressure loads causes distortions in the structure due to bending. The 3D FEA model provides integrated total displacements of each tubesheet bore location.

Table RAI4-1 is a summary of the maximum eccentricities and ΔDs for the Model F and Model D5 limiting plants as calculated based on the U_R (tubesheet radial displacement) results from the 3-D lower SG complex model.

Table RAI4-1: Summary of Model D5 and Model F NOP and SLB Eccentricity Results

SG Model	Elev.	Avg. Eccentricity Data		Max. Eccentricity Data		Avg. Δ D		Max. Δ D	
-	Above BTS[1]	NOP	SLB	NOP	SLB	NOP	SLB	NOP	SLB
-	in	in/in	in/in	in/in	in/in	in	in	in	in
F									
F									
F									
D5									
D5									
D5									
F									
D5									

a,c,e

Notes:
1. BTS is Bottom of the Tubesheet

The original Table RAI4-4 is provided here for convenience

			Eccentricity, *e*	Δ D, 0º	Δ D, 90º
Plant	Condition	Value	inch/inch	inch	inch
Byron	SLB	MAX			
Byron	SLB	MIN			
Byron	SLB	AVG			
Millstone	SLB	MAX			
Millstone	SLB	MIN			
Millstone	SLB	AVG			
Byron	NOP	MAX			
Byron	NOP	MIN			
Byron	NOP	AVG			
Millstone	NOP	MAX			
Millstone	NOP	MIN			
Millstone	NOP	AVG			

a,c,e

1.2 Discussion of the "Slice" Model

Clarify the nature of the finite element model ("slice" model versus axisymmetric SG assembly model) used to generate the specific information in Tables 6-1, 2, and 3 (and accompanying graph entitled "Elliptical Hole Factors") of Reference 6-15. What loads were applied? How was the eccentricity produced in the model? (By modeling the eccentricity as part of the geometry? By applying an axisymmetric pressure the inside of the bore?) Explain why this model is not scalable to lower temperatures.

The difference between initial and final eccentricity included in Table RAI4-2 needs to be explained. In particular, the exclusive use of the relationship between initial eccentricity and scale factor in calculating contact pressure needs to be justified.

Resolve the apparent inconsistency between Item 4 on page 25 and the statement below Figure RAI4-1 regarding how the model in Figure RAI4-1 is loaded.

Response:

The "slice model" is shown in Figure 6-9 of Reference 6-15 in WCAP-17071-P, WCAP-17072-P, WCAP-17091-P, and WCAP-17092-P.

The data in Tables 6-1, 6-2, and 6-3 of Reference 6-15 of the H* WCAP reports, are derived from this plane stress model ("slice model") developed in WECAN/PLUS and the contact pressure equation identified on page 6-87 of WCAP-17071-P, page 6-95 of WCAP-17072-P, page 6-91 of WCAP-17091-P and page 6-84 of WCAP-17092-P as described below.

For convenience Tables 6-1, 6-2, and 6-3 of Reference 6-15 are replicated below and re-named as follows:. Table 6-1 is renamed as Table RAI4-2, Table 6-2 is renamed as Table RAI 4-3, and Table 6-3 is renamed as Table RAI4-4.

The "initial" eccentricities (defined as $D_{MAX} - D_{MIN}$) applied in the "slice" model in Table RAI4-3 and Table RAI4-4 are directly incorporated into the model geometry. That is, the initial eccentricity is built into the model geometry. The eccentricity values in the model were assumed values for tubesheet tube bore deformation based on engineering judgment and prior experience.

In the "slice" model analysis, the tubesheet is assumed to have a thermal expansion coefficient of zero (0) in/in/°F and the tube material is assumed to have the appropriate ASME Code thermal expansion coefficient values. (The TS coefficient of thermal expansion is set to zero to provide a loading mechanism for the model. When a temperature is applied, the tube "grows" into the tubesheet collar. The temperature difference applied to the tube in the "slice" model was 500°F, for a total tube temperature of 570°F. [Applied 500°F + 70°F assumed room temperature]). The sole purpose of the development of the "slice" model was to provide a sensitivity study to relate the effects of assumed eccentricity ($D_{MAX} - D_{MIN}$) conditions to contact pressures from which the contact pressure ratios were developed. No attempt was made to

reproduce the contact pressures that would be calculated by the 2-D axisymmetric model that was previously used to develop the tubesheet displacements.

The "final" eccentricity ($D_{MAX} - D_{MIN}$) values in Table RAI4-3 and Table RAI4-4 were also determined using the "slice model": The final eccentricity values are the ($D_{MAX} - D_{MIN}$) results of applying the loading conditions on the slice model: The loads applied to the "slice" model were thermal loads only as follows:

0 psig - Primary Side Pressure
0 psig - Secondary Side Pressure
500 °F- Tubesheet ΔT
500 °F- Channel Head ΔT
500 °F- Shell ΔT

As discussed in Reference 6-15, Table RAI4-3 was constructed using the displacement results from the plane stress model analysis for the elliptical holes along with the contact pressure equations. The effective change in hole diameter was calculated as follows using a series of assumed scale factors:

$$\left[\qquad\qquad\right]^{a,c,e} \qquad \text{(RAI4-1)}$$

The ΔD_{MAX} and ΔD_{MIN} were taken from the radial and circumferential change in tube bore diameter in the "slice" model.

The corresponding contact pressure for each scale factor was then determined as follows:

$$\left[\qquad\qquad\right]^{a,c,e} \qquad \text{(RAI4-2)}$$

Equation RAI4-2 is a generic representation of how tube to tubesheet contact pressure is calculated in the H* integrator spreadsheet analysis. The equation is equivalent to the equation for P2 shown on page 6-87 in WCAP-17071-P, page 6-95 in WCAP-17072-P, page 6-91 in WCAP-10791-P and page 6-84 in WCAP-17092-P.

The scale factors for a given input eccentricity in Table RAI 4-3 result in contact pressure ratios using the thick shell equations that are equal to the contact pressure ratios calculated using the "slice" model for initial eccentricities (defined as $D_{MAX} - D_{MIN}$) equivalent to 0.0002, 0.0004, 0.0006 and 0.0008 inches, respectively, compared to the contact pressures for a circular hole ($D_{MAX} - D_{MIN} = 0$). These scale factors are identified in bold print in Table RAI4-3. The data for the scale factors as a function of "initial" eccentricity was fit by a third order polynomial equation provided on page 6-85 of WCAP-17071-P and page 6-86 of WCAP-17072-P.

Based on a review of Table RAI4-3 and Table RAI4-4, the scale factor [ ]^{a,c,e} is the appropriate scale factor for calculating a reduction factor for contact pressure of [ ]^{a,c,e} associated with an initial eccentricity of [ ]^{a,c,e} ((D_{MAX} – D_{MIN})/ [ ]^{a,c,e} inch) from the "slice" model. The scale factor of [ ]^{a,c,e} relates to a contact pressure reduction factor of [ ]^{a,c,e} and corresponds to an initial eccentricity of [ ]^{a,c,e} inch, and so forth.

The "final eccentricity" values corresponding to the same scale factors highlighted in bold in Table RAI 4-3 (and Table RAI4-4) are not used in determining the reduction in contact pressure because the resulting third order polynomial relationship between scale factor and eccentricity is bounded by the relationship for "initial eccentricity", i.e., the resultant scale factors, and hence the reduction in contact pressure due to eccentricity, would be less using the third order fit resulting from the "final" eccentricity values from Table RAI 4-3. For example, for an eccentricity of 1E-3 in/in, the scale factor is [ ]^{a,c,e} as compared to [ ]^{a,c,e} for the trend line associated with the "initial" eccentricity results. Figure RAI 4-1 illustrates this. This figure shows a comparison of the trend line analysis for "initial" eccentricity and "final" eccentricity. Referring to Equation RAI 4-1, larger scale factors result in a greater reduction in contact pressure due to eccentricity.

Table RAI4-2

Reproduced Table 6-1 of Reference 6-15

	Sleeve O.D.			Tube O.D.			
Eccentricity (inch)	Average[1]	Ratio[3]	Delta[1] [2]	Average[1]	Ratio[3]	Delta[1] [2]	a,c,e
0.0000							
0.0002							
0.0004							
0.0006							
0.0008							

Notes: This table is developed from the model shown in Figure RAI4-1, below.

1. The units of these columns are stress in psi.
2. The "delta" in this table refers to the maximum deviation from a constant value of the mean linearized radial stress around the tube bore.
3. The ratio is calculated by dividing the contact pressure between the tube and the tubesheet at a given eccentricity by the contact pressure between the tube and the tubesheet in a round tube bore (e=0.0). For example, the ratio of [ ]^{a,c,e} calculated in Table 6-1 is a ratio of the average contact pressure at an eccentricity of 0.0002 in of [ ]^{a,c,e} psi divided by the average contact pressure at an eccentricity of [ ]^{a,c,e} psi.

Table RAI4-3

Reproduction of Table 6-2 of Reference 6-15

Primary Pressure		0	psig
Secondary Pressure		0	psig
Tubesheet Delta T		500	°F
Shell Delta T		500	°F
Channel Head Delta T		500	°F
Sleeve OD Delta D	[	]a,c,e	in
Tube ID Delta D	[	]a,c,e	in
Tube OD Delta D (Thermal)	[	]a,c,e	in
Sleeve/Tube Interaction Coefficients	[	]a,c,e	
Tube/Tubesheet Interaction Coefficients	[	]a,c,e	

Eccentricity		(1)	(2)	(3)	(4)	(5)	(6)
Initial (inch)	Final (inch)	Max/Min Combination	Hole Delta D (0 Deg)	Hole Delta D (90 Deg)	S/T Contract Pressure	T/TS Contact Pressure	Ratio
0.0000		Minimum **Average** Maximum					
0.0002		Minimum Average Maximum					
0.0004		Minimum Average Maximum					

a,c,e

Table RAI4-3 (Cont'd.)

Eccentricity [a,c,e]	(1)	(2)	(3)	(4)	(5)	(6)
0.0006	Minimum					
	Average [a,c,e]					
	Maximum					
0.0008	Minimum					
	Average [a,c,e]					
	Maximum					

[a,c,e]

*Note: The values in **Bold** identify the source data for Table RAI4-3*

Table RAI4-4

Reproduction of Table 6-3 of Reference 6-15

Nominal Hole Diameter [ ] [a,c,e]

Initial Delta Dia (in)	Eccentricity[(1)] Initial (in/in)	Final (in/in)	Max/Min Factor	Pressure Ratio
0.0000				
0.0002				
0.0004				
0.0006				
0.0008				

a,c,e

(1) These values are the values for initial and final eccentricity from Table RAI4-2 are divided by the nominal tubesheet hole diameter [ ] [a,c,e]

[

]a,c,e

a,c,e

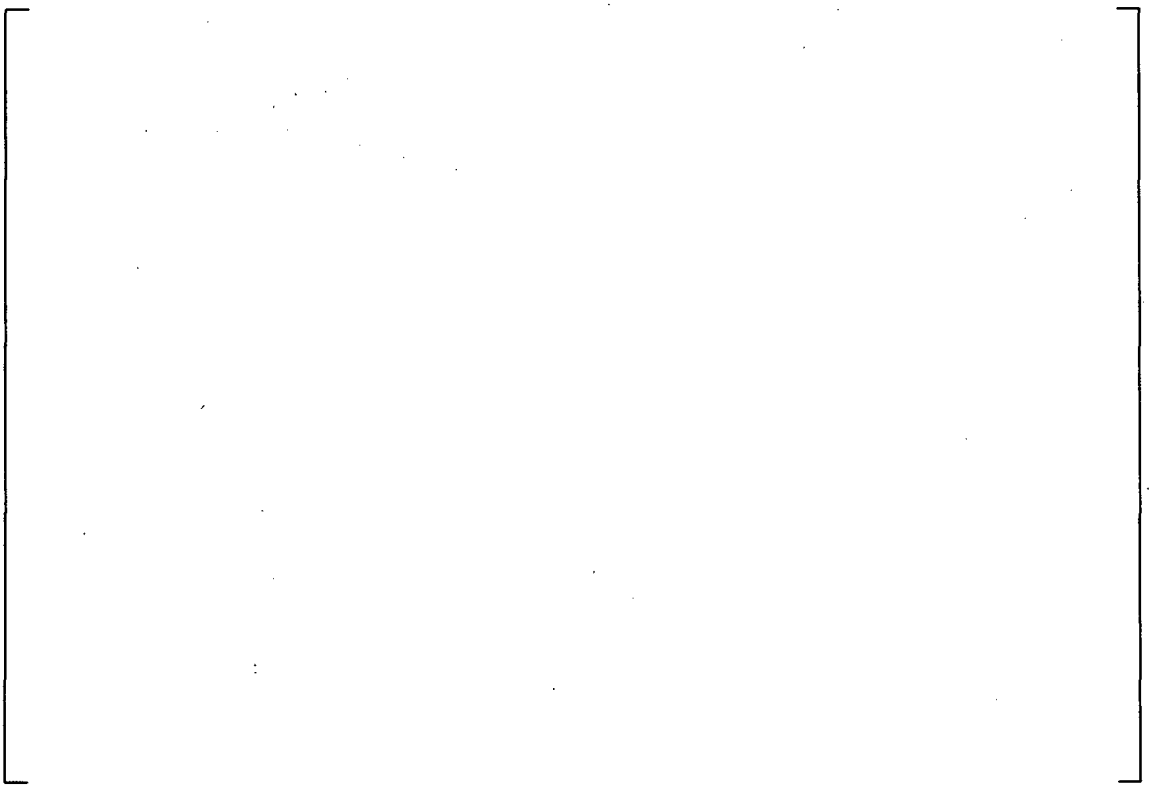

Figure RAI4-2: Scale Factor Comparison (Initial versus Final Eccentricity)

The method for calculating the contact pressure for using the "old" method for the Model F SGs (all plant conditions) and the Model D5 SGs (NOP and FLB conditions) and the "new" method for calculating the contact pressure the Model D5 SGs only (SLB conditions) are described below:

Old Method (Reference 6-15):

1. The U_R used in the calculation of the circumferential and radial ΔD is based on the linearly scaled 2D axisymmetric FEA model (3-D model for the current H* analysis) of the lower SG complex

2. The circumferential and radial ΔD's are used in the scale factor (SF) equation to determine the ΔD_{hole} (see equation RAI4-1) that is used to determine the reduction in contact pressure as a function of eccentricity (e), equation RAI4-2.

3. The relationship between 11D and e is based on the 2-D plane model shown in Figure 6-9 of SM-94-58, Rev.1.

4. The model in Figure 6-9 of SM-94-58, Rev.1 includes the initial applied eccentricities (D_{MAX} – D_{MIN}) geometry definition of the model.

5. The "slice" model provides the input for using the SF relationship (Eqn. RAI4-1). The SF is determined by comparing the "slice" model results to the axisymmetric model results for a TS collar and tube model at a given radius in the TS over the full thickness of the TS.

6. The result is then used to calculate the reduction in contact pressure as a function of TS elevation and radius due to TS displacement and tube bore eccentricity. This is appropriate because the conditions for the Model F SG and Model D5 SG (NOP and FLB conditions) are within the range of data for which the scale factor relationship is applicable.

New Method (WCAP-17071-P, WCAP-17072-P):

1. The U_R used in the calculation of the circumferential and radial ΔD comes from a 3-D FEA model of the lower SG complex with condition-specific inputs applied.

2. The circumferential and radial ΔD's are compared to determine the maximum ΔD that will give the maximum reduction in contact pressure as a function of eccentricity (e).

3. The relationship between ΔD and e is based on the 2-D [ ]^{a,c,e} model shown in WCAP-17071-P and WCAP-17072-P, section 6.2.5. The model is shown in Figure 6-49 of the WCAP reports. The range of eccentricity used in this study conservatively exceeds the values of tube bore eccentricity calculated from the perforated TS model in Section 6.2.4.

4. The model in Figure 6-49 of the H* WCAP reports applies boundary conditions to the outer edge of the tube pitch material and does not directly affect the material that is deforming in the tube and tubesheet cell.

5. The TS deformations and tube to tubesheet contact pressure results that produce the maximum reduction in contact pressure at the minimum value of TS tube bore eccentricity are then fit with a linear relationship.

6. The result of the linear relationship is used to determine the reduction in contact pressure between the tube and the tubesheet directly. There are no intermediate equations or results.

A correct prediction of contact pressure loss requires the knowledge of both the proper values of D_{MAX} and D_{MIN} associated with the different pressure and temperature conditions at a given tubesheet radius and elevation as well as the value of eccentricity. The values of D_{MAX} and D_{MIN} are a function of the radial deflection of the tubesheet, U_R, as determined by the finite element analysis model (which previously was a 2-D axisymmetric model of the SG lower

assembly and at present, is a 3-D model of the SG lower assembly). The results from the "slice" model cannot be linearly scaled to lower temperatures because the method of super-position has been shown during the development of the current H* analysis to not apply to the non-linear combination of materials and loading in the lower SG complex. This conclusion led to the development of the 3D FEA model that is the reference model for the H* analysis. A discussion of this is provided in Section 6.1.2 of WCAP-17071-P and WCAP-17072-P.

1.3 Discussion of the Unit Cell Model to Calculate Contact Pressures

The "Unit Cell" model is extensively discussed in Section 6.2.5 of the H* WCAPs (References 8 and 9). The specific goal of this model was to determine if tube to tube contact would remain when the tubesheet is deformed due to operating loads. An equivalent tubesheet cell is modeled, that is, a tubesheet bore with surrounding tubesheet material, and a tube in the tubesheet bore (see Figure 6-48 of the H* WCAPs). For the primary purpose of this model – to study if tube-to-tubesheet contact is present during the limiting tubesheet deformations – the model was initialized by simulating the tube expansion process. The expansion process was conservatively simulated by applying a low value of expansion pressure [ ]^{a,c,e} inside the tube, resulting in initial tube to tubesheet contact, and then removing the tube expansion internal pressure. The calculated dilation of the tubesheet bore due to the simulation of the tube expansion is [ ]^{a,c,e} inch for all models of SG considered.

As discussed in Section 6.2.5 of the H* WCAP reports, the operating pressure loads, were applied to the initialized model in a sequential manner, and the resulting contact pressures were calculated when a range of displacements (termed "E-bar") were applied as boundary conditions to the model. Figure RAI4-2 shows the updated sequential loading (includes application of thermal loads) of the model and relates it to the steps discussed in Section 6.2.5 and Tables 6-18 and 6-19 of the H* WCAPs. The "E-bar" values shown as the displacement inputs on Tables 6-18 and 6-19 in the H* WCAP reports are uni-directional displacements (in inches) that are NOT the same as eccentricity and also not the same as ΔD. (Eccentricity is defined as the difference between the maximum and minimum diameters of a bore divided by the nominal diameter of the bore. The units of eccentricity are inch/inch.) The displacement inputs applied to the unit cell model are assumed values that based on prior analyses that envelope the expected tubesheet displacement for all of the applicable operating conditions. It is important to note that the unit cell model as described in Section 6.2.5 of the H* WCAP reports utilizes boundary conditions chosen to minimize the tube-to-tubesheet contact pressures for the applied relative displacements.

To interpret the results from the unit cell model properly, the following must be observed:

- To address if tube to tubesheet contact continues for all the assumed tubesheet displacements, the appropriate reference condition is the initialized condition (after Step 4) of the model that simulates a tube expanded in the tubesheet bore.

- To compare the results of the unit cell model with the 3D FEA model, the appropriate reference condition of the unit cell model is the initial model (Step 0) without the tube expansion simulated and thermal loads must be included.

Figures RAI4-3 and RAI4-4 show the average tubesheet bore dilation (ΔD) as a function of tubesheet relative displacement (E-bar) for the Model F and Model D5. The average tube bore dilation at zero E-bar input is the result of the temperature and pressure loading of the unit cell model. Initially, application of the displacement input "E-bar" results in more significant hole dilation, but rapidly takes on a shallower slope as the applied displacement increases. The curves are characteristically the same for the Model F and Model D5 steam generators and also for the different operating conditions, NOP and SLB, for the different models of SGs.

Similarly, Figures RAI4-5 and RAI4-6 show the tubesheet bore eccentricity "e" as a function of tubesheet relative displacement (E-bar) for the Model F and Model D5. Eccentricity initially increases with application of the displacement boundary condition (E-bar) simulating the load due to pressure differential across the tubesheet, but the rate of increase decays with increasing E-bar. A significant difference is noted between NOP and SLB conditions at large values of E-bar. This difference reflects the fact that the uniform growth of the tube bore hole due to increased temperature overwhelms the effect of application of the displacement boundary condition (E-bar) on tubesheet bore eccentricity. During the SLB event, the temperature is decreased and the differences in D_{MAX} and D_{MIN} remain more significant as the displacement boundary condition is increased, although the rate of increase in the difference between D_{MAX} and D_{MIN} is reduced at some point. . Eventually, at NOP conditions, the difference between D_{MAX} and D_{MIN} tends to become decrease even though a greater displacement (E-bar) is applied, leading to a reduction of eccentricity "e."

Figures RAI4-7 and RAI4-8 show the contact pressure as a function of tubesheet relative displacement (E-bar) for the Model F and Model D5 for both NOP and SLB conditions based on the unit cell model. As expected, both NOP and SLB contact pressure decrease with increasing displacement inputs, ultimately going to zero at a very large value of applied displacements. It is to be noted that the maximum displacement assumed is significantly greater than would be predicted by the 3D FEA model. Over the entire range of assumed displacement conditions, the SLB contact pressure exceeds that for NOP conditions.

Table RAI4-5 summarizes the eccentricity, ΔD and predicted contact pressure using the unit cell model for various values of applied displacement (E-bar) for both the model F and Model D5 SGs. The true eccentricity ($[D_{max}-D_{min}]/D_{nom}$) is shown for the applied displacement, E-bar. Table RAI4-5 also provides a comparison of the ΔD predicted by the unit cell model for the two reference conditions noted above, that is, for the total ΔD from the model without the simulated tube expansion (reference step 0 in Table 6-18) and for the initialized case with the tube expansion simulated (reference step 4 in Table 6-18).

Further, Table RAI4-5 provides a summary of contact pressures between the tube and the tubesheet for various applied values of E-bar for the Model F and Model D5 SGs. The "Modified Contact Pressure" is the "Raw Contact Pressure" from the unit cell model adjusted for the actual tube expansion process ([ ]^{a,c,e} psi compared to the simulation at [ ] ^{a,c,e} psi) real Model F and Model D5 geometry and more realistic operating conditions of pressures and temperatures. For all cases of applied displacement, positive contact pressure remains between the tube and tubesheet. It should be noted that the largest value of applied displacement (E-bar) is well in excess of the displacement predicted by the 3D FEA model.

Table RAI4-6 provides similar data to that in Table RAI4-5, except that the data is based on the 3D FEA model.

Comparison of Tables RAI4-5 and RAI4-6 leads to the following observations:

1.The ΔDs from the 3D FEA model are significantly less than the corresponding ΔDs from the unit cell model from the unloaded to the fully loaded condition (i.e., from step 0 to step 9) for both NOP and SLB conditions. This leads to the conclusion that the unit cell model displacement results and contact pressure predictions conservatively represent the reference 3D FEA model results.

2. The eccentricities from the unit cell model are generally comparable to those from the 3D FEA model. A more exact comparison is difficult based on the available data; however, it is clear that the actual range of eccentricities from the 3D FEA model was adequately addressed by the unit cell model.

3. The method of Reference 6-15 of the H* WCAP report for adjusting contact pressure provides acceptable results for all conditions except the SLB condition for the Model D5 SGs The method of Reference 6-15 significantly under-predicts contact pressure for the Model D5 SLB conditions. Referring to Figure RAI4-6, the method for calculating the reduction in contact pressure defined by the White Paper, when adjusted for temperature effects, shows that SLB contact pressure is increased relative to normal operating conditions.

Table RAI4-5
Eccentricity, Contact Pressure and ΔD Results from Unit Cell Model

		Square Cell Results		Square Cell Results		Square Cell Results		Square Cell - Average Delta D				
		Eccentricity		Raw Contact Pressure[1]		Modified Contact Pressure[1]		Step 0[2] - Step 9[3]		Step 4[4] - Step 9[3]		
SG Model	"E bar"	NOP	SLB	NOP	SLB	NOP	SLB	NOP	SLB	NOP	SLB	a,c,e
-	in	in/in	in/in	psi	psi	psi	psi	in	in	in	in	
F												
F												
F												
F												
D5												
D5												
D5												
D5												

Notes:
1. Accounts for expansion pressure and geometry.
2. See Section 6.2.5 H* WCAP. Step 0 is the condition of the unit-cell model prior to any modifications for tube expansion, loading, etc.
3. See Section 6.2.5 H* WCAP. Step 9 is the condition of the unit cell model after all loading conditions have been applied.
4. See Section 6.2.5 H* WCAP. Step 4 is the initialized condition of the Unit Cell model after tube expansion has been simulated.

Table RAI4-6
Eccentricity, Bore Dilation and Contact Pressure from 3D FEA Model

SG Model and Contact Pressure Reduction Model	Hstar Analysis Eccentricity		Hstar Analysis Avg. Contact Pressure		Hstar Analysis - Avg. Δ D No Load to Operating	
	NOP	SLB	NOP	SLB	NOP	SLB
	in/in	in/in	psi	psi	in	in
F - Ref. 6-15						
Limiting Radius - F - Ref. 6-15						
D5 - Ref. 6-15						
D5 - White Paper						
Limiting Radius - D5 - Ref. 6-15						
Limiting Radius - D5 - White Paper						
F - Updated Model (1)						
D5 - Updated Model (1)						

a,c,e

(1): Updated Model Results based on estimates from approximate values in finite element analysis and do not reflect the result of a regression analysis.

Figure RAI4-2
Unit Cell Model and Loading Sequence

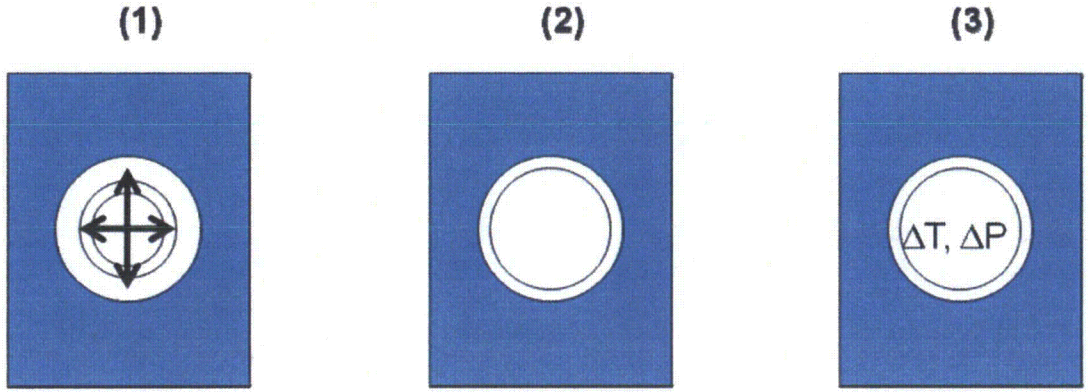

Step 0
ΔP = 0
ΔT = 0
Unexpanded Tube
e = 0
e bar = 0

Step 5
ΔP = 0
ΔT = 0
Expanded Tube
e = 0
e bar = 0

Step 6-9
ΔP > 0
ΔT > 0
Expanded Tube
e > 0
e bar > 0

Loading Steps:
0. Initial Model
1. Initial Tube to TS gap
2. Pressurize tube to 16ksi
3. Pressurize tube to 28ksi
4. Release Pressure on Tube
5. Apply $\Delta T^{(1)}$
6. Apply "E-bar"
7. Apply ΔP=[ ]^{a,c,e} psi
8. Apply ΔP=[ ]^{a,c,e} psi
9. Apply ΔP=[ ]^{a,c,e} psi

Notes: (1) The application of the unit cell model in support of Tables 6-18 and 6-19 does not include application of ΔT.

a,c,e

Figure RAI4-3
Relationship between "E-bar" and ΔD; Model F

a,c,e

Figure RAI4-4
Relationship between "E-bar" and ΔD; Model D5

[a,c,e]

Figure RAI4-5
Relationship between "E-bar" and Eccentricity "e"; Model F

[a,c,e]

Figure RAI4-6
Relationship between "E-bar" and Eccentricity "e"; Model D5

a,c,e

Figure RAI4-7
Relationship between "E-bar" and Contact Pressure; Model F

a,c,e

Figure RAI4-8
Relationship between "E-bar" and Contact Pressure; Model D5

2.0 Comparison of Slice Model and Unit Cell Model Results

The basis for applying the correlation for scale factor outside an "eccentricity" range of between 1E-3 to 1E-4 inch in the calculation of contact pressure needs to be further explained. Values for displacements included in Table 6-18 (of WCAP-17071) suggest that contact pressure may be lost at displacement ranging between 1E-3 in to 1E-4 in.

Response:

Interpretation of the displacements noted in Table 6-18 of the WCAP reports was clarified in the prior response, Section 1.3. The values noted in the column titled "Displacement Total" refer to the condition of the unit cell model after Step 4 of the loading sequence (See Figure RAI4-2). When the true reference condition (Step 0) for total displacement is considered, the values of total displacement are significantly larger as noted previously.

Westinghouse agrees that the derivation of the fit in Reference 6-15 is non-intuitive and limited in its application. However, the results of applying the fit described in reference 6-15 are acceptable relative to a best case finite element model (unit cell with thermal and ΔP loading) for the reasons described below.

Westinghouse also agrees that the fit that describes the reduction in contact pressure for the steam line break condition in the Model D5 White Paper does not account for the reduction in contact pressure due to tube bore dilation in the same manner as the fit described in Reference 6-15. The results of using the fit described in Reference 6-15 also match the expected trend from a best case finite element model. See the response to b.4 below for more details.

A series of tubesheet tube bore eccentricities were applied to the tubesheet cell model and combined with different pressure and temperature loads. The average, maximum and minimum values of the tube-to-tubesheet (T/TS) contact pressures around the circumference of the tube were reported. The values of tubesheet relative displacement, pressure and temperature that were used in the analysis are summarized in the table below.

Input Conditions for Unit Cell Model (no correlation implied)		
$\bar{e}$	Internal Pressure	Temperature Difference
in	ΔP, psi	ΔT, °F a,c,e
0.00	[	]
2.0E-04		
4.0E-04	[	]

Normal operating (NOP) conditions in the Model D5 and Model F steam generators are represented by a ΔP of [ ]^{a,c,e} psi and a ΔT of [ ]^{a,c,e} °F. Main steam line break (SLB) conditions in the Model D5 are represented by a ΔP of [ ]^{a,c,e} psi and a ΔT of [ ]^{a,c,e} °F. The value of ΔP in the tubesheet cell can change as a function of elevation in the tubesheet due to the distribution of crevice pressure. The results of the study include the data for a depth ratio of 0.9 which is an elevation roughly 2 inches below the top of the tubesheet. The values of ΔP represented in this study account for the region of interest near the top of the tubesheet where the maximum eccentricity in the tubesheet is expected and where the crevice fluid is transitioning from the crevice conditions to the secondary side fluid conditions. The region roughly 2 inches below the top of the tubesheet is also where a significant portion of the T/TS contact pressure develops so it is a good indicator of trends in the effect that different operating conditions have on the contact pressure.

The original results in section 6.2.5 of WCAP-17071-P were used to verify that the reduction in T/TS contact pressure as a function of tubesheet tube bore eccentricity was appropriate for the Model F SG. The original relationship that is used to define the reduction in T/TS contact pressure as a function of eccentricity is described in section 6.3 of WCAP 17071-P and WCAP 17072-P. However, the result of applying the fit described in section 6.3 to the Model D5 SG during SLB was shown to be inconsistent with the expected trend from the more detailed analysis described in section 6.2.5. The results of section 6.2.5 were then used to define a new relationship between the reduction in T/TS contact pressure and tube bore eccentricity. This new relationship is described in the Model D5 White Paper (Reference 12). Figure RAI4-8 shows the result of applying the new relationship to the Model D5 SLB conditions (i.e., White Paper results, Reference 12) in comparison with the results from the old 3rd order polynomial relationship. Because the tubesheet temperature induced hole dilation, potentially the most significant factor in contact pressure reduction, was not considered in the Model D5 condition results, a third curve was added to the figure titled "Model D5 FEA trend." This curve represents the most accurate calculation of the contact pressure ratio.

Figure RAI4-9 shows the contact pressure ratio (PC_{SLB}/PC_{NOP}) as a function of tubesheet relative displacement, E-bar. It is clear from Figure RAI4-9 that the results of using the old fit for the Model D5 SLB are inconsistent with the more detailed analysis. At SLB conditions, the tubesheet bore dilation is relatively larger than at NOP conditions due to the increased bending of the TS and decreased thermal expansion. Therefore, it is expected that the T/TS contact pressure ratio should increase by a factor of at least [ ]^{a,c,e} (see Figure RAI4-9) when going from NOP to SLB. It is also expected that the tube to tubesheet contact pressure should decrease with increasing tube bore eccentricity. The H* results using the old fit for the Model D5 clearly do not follow either expectation from the detailed analysis. However, when the new fit results are applied to the H* calculation process the relationship between T/TS contact pressure in the Model D5 is much more reasonable and follows the expected trend from the more detailed analysis.

The Model F H* contact pressure results, using the old fit, are well within the range predicted by the more detailed analysis in section 6.2.5 and the additional work described in this RAI response. See Figure RAI 4-10 below. This means that the old fit is appropriate to use for the

Model F NOP and SLB conditions and the NOP condition in the Model D5 SG. The results of using the fit described in Reference 6-15 match the expected trend from a best case finite element model for the NOP and SLB conditions for the Model F SGs and NOP conditions for the Model D5 SG.

To further address the concern that contact pressure may be lost at displacements ranging between 1E-3 in and 1E-4 in, the "Unit Cell" model is extensively discussed in Section 1.3 of this response above.

a,c,e

Figure RAI 4-9

a,c,e

Figure RAI 4-10

2.1 Calculation Basis for Contact Pressure Reduction Factors

Provide the calculation basis for the upper and lower curves provided in Figure RAI 4-2

Response:

The original figure RAI4-2, referred to in the question, is reproduced here as RAI4-10 to provide the foundation for the question and the response. Note that the scale of the y-axis has been corrected as discussed in the meeting on August 17, 2009.

a,c,e

Figure RAI4-10 (original Figure RAI4-2)

The upper curve in the figure above is based on the data from the following table:

Eccentricity (ΔDmax-ΔDmin) (in)	Reduction in Contact Pressure (psi)(1)	Normalization Basis (psi)	Contact Pressure Reduction Factor(psi/psi)
0	0	1200	0
2E-4	[ ]^{a,c,e} psi		[ ]^{a,c,e}
4E-4	[ ]^{a,c,e} psi		[ ]^{a,c,e}
5E-4	[ ]^{a,c,e} psi		[ ]^{a,c,e}
6E-4	[ ]^{a,c,e}		[ ]^{a,c,e}
Notes: (1) Contact stress reductions are based on the values on Table RAI4-3			

Referring to Table RAI 4-3, the contact pressure for a round tube bore hole is calculated to be [ ]^{a,c,e} psi (Ratio = 1.0). The contact pressure for a tube bore hole that results in a contact pressure ratio reduction of [ ]^{a,c,e} (Ratio = [ ]^{a,c,e}), which corresponds to an eccentricity of 2E-4 inch, is [ ]^{a,c,e} psi. The absolute reduction in contact pressure is [ ]^{a,c,e} psi.

The total reduction in contact pressure using the new model is approximately [ ]^{a,c,e} psi (see Figure 6-69 of WCAP-17072-P). To plot the absolute reduction in contact pressure of [ ]^{a,c,e} psi for an eccentricity of 2E-4 on Figure RAI4-10, the value is normalized by the total reduction in contact pressure of [ ]^{a,c,e} psi from the new method. This value represents a reduction in contact pressure of [ ]^{a,c,e}.

Again, referring to Table RAI 4-3, the contact pressure for a round tube hole is calculated to be [ ]^{a,c,e} psi. The contact pressure for a tube bore hole that results in a contact pressure ratio reduction of [ ]^{a,c,e} (Ratio = [ ]^{a,c,e}), which corresponds to be eccentricity of 4E-4 inch, is [ ]^{a,c,e} psi. The absolute reduction in contact pressure is [ ]^{a,c,e} psi.

Again, the total reduction in contact pressure using the new model is approximately [ ]^{a,c,e} psi (see Figure 6-69 of WCAP-17072-P). To plot the absolute reduction in contact pressure of [ ]^{a,c,e} psi for an eccentricity of 4E-4 on Figure RAI4-10, the value is normalized by the total reduction in contact pressure of [ ]^{a,c,e} psi from the new method. This value represents a reduction in contact pressure of [ ]^{a,c,e}.

The same calculation was completed for an eccentricity of 6E-4 in. The value for 5E-4 in is an interpolated value between 4 E-4 in and 6E-4 in.

The bottom curve in the figure above is generated using the 3rd order polynomial fit. The results are summarized in the following table:

E, eccentricity (in)	T/TS Contact Pressure Reduction (psi)	Normalized Contact Pressure Reduction
6.36E-07	[ ]^{a,c,e}	[ ]^{a,c,e}
5.53E-05	[ ]^{a,c,e}	[ ]^{a,c,e}
3.16E-04	[ ]^{a,c,e}	[ ]^{a,c,e}
5.69E-04	[ ]^{a,c,e}	[ ]^{a,c,e}
9.07E-04	[ ]^{a,c,e}	[ ]^{a,c,e}

2.2 Conservatism of 3rd Order Polynomial Fit from WCAP Reference 6-15

Provide the basis for why the ΔD_{hole} adjustment for contact pressure made using the old model remains conservative.

Response:

The key conclusions from the comparison of the Reference 6-15 analysis, the WCAP results and the results of the square cell tubesheet model are:

1.) The fit described in Reference 6-15 of the H* WCAP reports is conservative when applied to the NOP condition in both the Model D5 and Model F SG. The fit tends to under-estimate the contact pressure during NOP by as much as [ ]^{a,c,e} psi to [ ]^{a,c,e} psi) for the Model F SG and as much as [ ]^{a,c,e} % for the Model D5 SG ([ ]^{a,c,e} psi to [ ]^{a,c,e} psi) (see Table RAI4-6).

2.) The fit described in Reference 6-15 of the H* WCAP reports is comparable when applied to the SLB condition in the Model F SG. The fit described in the Model D5 White Paper tends to over-estimate the contact pressure, by as much as [ ]^{a,c,e} %, during SLB ([ ]^{a,c,e} psi to [ ]^{a,c,e} psi) because the White Paper does not fully account for the change in tube bore diameter during the transient.

3.) The fit described in Reference 6-15 of the H* WCAP reports significantly under-estimates the contact pressure, by as much as [ ]^{a,c,e} %, during the D5 SLB condition (from [ ]^{a,c,e} psi to [ ]^{a,c,e} psi).

4.) The square cell tubesheet finite element model shows an increase in contact pressure when going from NOP to SLB conditions in both the D5 and F SGs.

5.) Using the results from the square cell model to estimate the magnitude of the contact pressure reduction from the change in tube bore diameter calculated using the 3D finite element results from the lower SG tubesheet complex model show that the contact pressure still increases when going from NOP to SLB conditions in both the Model F and Model D5 SG.

The results of this analysis show that NOP contact pressures that define H* in the Model F and Model D5 SG are conservative and that a more realistic model of contact pressure reduction as a function of tube bore deformation (including both dilation and eccentricity) would predict an increase in tube to tubesheet contact pressure at SLB conditions compared to NOP conditions.

(See also Section 2.3)

2.3 SLB vs. NOP Contact Pressures

Provide an appropriate basis for demonstrating that joints tighten during a postulated SLB event. Why is it acceptable to compare the contact pressures calculated using the original model for NOP to the contact pressures calculated using the new model for SLB for the Model D5 SGs?

Response:

Table RAI4-5 provides a summary of contact pressures between the tube and the tubesheet for various applied values of E-bar for the Model F and Model D5 SGs. Comparison of the eccentricity values calculated using the unit cell model (see Table RAI4-5) with the eccentricity values calculated from the 3D FEA model (see Table RAI4-1) shows that the eccentricities from both models are comparable. It is not reasonable to expect exact matches of numbers between the two models, however, the order of magnitude of the calculated eccentricities is the same. Given that the two structural models provide similar eccentricities, the unit cell model shows that for these eccentricities, positive contact pressure exists between the tubes and the tubesheet for the entire range of displacements considered. Further, the results show that the contact pressures at SLB conditions exceed those at NOP conditions (See Table RAI4-6). See also the discussion in Section 2.4 below.

2.4 Relative Conservatism of "Old" and "New" Fit

If both old and new models are conservative, is there an appropriate basis to show the relative conservatism of the methods?

Response:

As noted above in Section 1.3 of this response, tube bore dilation is a more significant factor in determining tube-to-tubesheet contact pressure at higher temperatures and the effect of eccentricity on contact pressure is reduced at higher temperatures. The methodology for addressing the effect of eccentricity on contact pressure discussed in Reference 6-15 and utilized in WCAP-17071-P, WCAP-17072-P, WCAP-17091-P and WCAP-17092-P reflects this fact and it, therefore, provides acceptably accurate contact pressure results at higher temperatures (i.e., for all conditions except the "colder" SLB condition). This includes NOP, SLB (higher temperature, > 400°F, and FLB, where appropriate).

Also, as noted in Section 1.3 of this report, the effect of eccentricity on contact pressure loss is a more significant factor at the lower SLB temperatures for the Model D5 SG, but tube bore dilation due to temperature and pressure needs to be considered (which was not addressed in the "new" method, a.k.a the White Paper method discussed in WCAP-17072-P or 17091-P). Moreover, the original 3rd order polynomial fit significantly over-predicts contact pressure loss during the "colder" Model D5 SLB transient (and Model 44F two loop plant SLB).

Therefore, a more detailed model for contact pressure during a postulated SLB was developed. Referring to Table RAI4-6, it shows that contact pressure increases during a SLB event ([ ]^{a,c,e} psi) relative to NOP ([ ]^{a,c,e} psi) with primary and secondary side temperatures as low as 212°F when comparing contact pressures for NOP conditions for the unit cell to contact pressures for SLB for the unit cell.

Again, referring to Table RAI4-6, it has been shown when comparing contact pressures for NOP conditions for the unit cell to contact pressures for SLB for the unit cell for the Model F SG (higher temperature SLB conditions), that contact pressure increases during a postulated SLB (from [ ]^{a,c,e} psi at NOP to [ ]^{a,c,e} psi at SLB).

3.0 Comparison of 3D FEA and Unit Cell Model Results

The eccentricities included in Table RAI 4-4 appear larger than anticipated. Need to confirm that positive contact pressure exists around the entire circumference of the tube and state this clearly in the response.

Response:

Comparison of the eccentricity values calculated using the unit cell model (see Table RAI4-5) with the eccentricity values calculated from the 3D FEA model (see Table RAI4-1) shows that the eccentricities from both models are comparable. It is not reasonable to expect exact matches of numbers between the two models, however, the order of magnitude of the eccentricities calculated is the same. Given that the two structural models provide similar eccentricities, the unit cell model shows that for these eccentricities, positive contact pressure exists between the tubes and the tubesheet for the entire range of displacements considered. Further, the results show that the contact pressures at SLB conditions exceed those at NOP conditions.

4.0 Additional Background Information For Key Questions and Issues

RAI#4 evolved in several stages, each stage building on the prior stage. Reference 10 provided additional questions to augment those that were provided by Reference 5. Responses were prepared and were discussed in a telephone conference on August 11, 2009. During this telephone conference, additional questions were raised as identified in the introduction of this document. The following are responses that were provided in response to Reference 10 that were discussed in the August 11, 2009 telephone conference. They are historical in nature and are provided to complete the record of information provided in response to the NRC request for additional information.

4.1 Comparison of "Old and New" Relationship for Reduction in Contact Pressure and Eccentricity

In Figure 2 of the White Paper, add a plot for original relationship between reductions in contact pressure and eccentricity as given in Reference 6-15 in the graph accompanying Table 6-3. Explain why this original relationship remains conservative in light of the new relationship. Explain the reasons for the differences between the curves.

In order to superimpose the results of the "old" and "new" analyses for reduction in contact pressure related to eccentricity, the data for the "old" method must be normalized in the same fashion that Figure 2 has been normalized. The plot of contact pressure reduction included in

Figure 2 of the White Paper represents the total reduction in contact pressure associated with a given eccentricity. The information from Table 6-3 represents the ratio of the contact pressure calculated at a given eccentricity divided by the contact pressure calculated for a tubesheet bore with no eccentricity. For the new analysis, the total reduction in contact pressure for the eccentricities ($D_{MAX} - D_{MIN}$) for a range of up to [ ]^{a,c,e} inch is determined to be [ ]^{a,c,e} psi. For the old analysis, the total reduction in contact pressure for eccentricities in the same range is calculated to be [ ]^{a,c,e} psi. The normalization basis is the same for both curves on the figure.

Figure RAI4-11, showing the normalized results as discussed during the August 17, 2009 meeting, is provided below. (Figure RAI4-11 is the same as Figure RAI4-10 in Section 2.1 of this document, except that the values of the "Old Polynomial Results" have been corrected on Figure RAI4-10 by a factor of 2 as discussed in the August 17, 2009 meeting.) The curve labeled "Old" Model Results is based on the data from Table RAI4-3 (Table 6-2 of Reference 15 of the WCAP report). The curve labeled "New" Model reproduces Figure 2 in the White Paper (Reference 12). The curve labeled "D5 SLB Polynomial Fit" are the results when the eccentricity data and ΔD_{hole} for the Model D5 SLB condition are applied directly to the polynomial fit, equation 6-8 in WCAP-17072-P and similar equation on page 6-85 in WCAP-17071-P. The latter curve is based on the maximum displacement conditions at the top of the tubesheet for the Model D5.

The curve labeled "Old Model Results" (top curve on Figure RAI4-11) is misleading relative to making an assessment of the conservatism of the new analysis method compared to the old analysis method. Unlike the new analysis method, which is only applied to the SLB case for the Model D5 SGs, the old analysis method has not been applied as a linear function as represented in the figure as the uppermost curve (solid squares). In reality, the old data fit (top curve on Figure RAI4-11), which is a 3rd order polynomial fit, when extrapolated significantly outside its supported data range (i.e., at temperatures either significantly above or below 500°F), provides physically unrealistic results as shown on Figure RAI4-11 (bottom curve, Δ-symbols). The Model D5 SLB condition puts the tubesheet at a nearly uniform temperature of less than 300°F, which is far outside of the range for which the eccentricity relationship was developed in Reference 6-15 in the WCAP reports.

The original relationship remains conservative because it predicts greater reduction of tube to tubesheet contact pressure than the new method for all operating conditions. However, the original relationship is only valid when ΔD_{min} and ΔD_{max} are within [ ]^{a,c,e} % and eccentricity is within [ ]^{a,c,e} inch to [ ]^{a,c,e} inch range, (i.e., the basis of the original fit).

The maximum tube bore distortions occur at the top of the tubesheet. The results from applying the old fit for the relationship versus the new fit for the relationship for the Model D5 SLB tubesheet displacements and contact pressures are shown in Table RAI4-7. The tube-to-tubesheet (T/TS) contact pressure result due to thermal expansion of the tube and the pressure expansion of the tube including the effect of the crevice pressure distribution, is the same in the both the "old" and "new" cases in the Table RAI4-7 .

Table RAI4-7
Summary of Model D5 SLB Contact Pressure Results for Different Eccentricity Fit Relationships

Model D5			T/TS P_{CON} Reduction		T/TS P_{CON}	
Condition	Value	Eccentricity	Old	New	Old	New
SLB	Avg	[				
SLB	Max					
SLB	Min					] a,c,e

The results in Section 6.2.4 of WCAP-17071-P and WCAP-17072-P show that the average expected tubesheet-tube-bore eccentricity is on the order of [ ]^{a,c,e} inch. The results in Table RAI4-7 show that the old method of calculating the reduction in contact pressure due to tubesheet-tube-bore eccentricity and change in diameter is conservative for larger values of eccentricity and ΔD (predicts greater decrease in contact pressure) than the new fit. However, it is inappropriate to use the old method at smaller values of eccentricity and ΔD because it provides physically impossible results (see Table RAI4-7). For example, the "old" method predicts a larger decrease in contact pressure for a smaller eccentricity on the order of 10^{-7} inch than for a larger eccentricity on the order of 10^{-3} inch. The "new" method, by comparison, predicts a slightly positive increase in contact pressure for an eccentricity of 10^{-7} inch and a large reduction in contact pressure for an eccentricity of 10^{-4} inch or greater, a physically realistic result. The reason that the "old" method predicts such a different reduction in contact pressure for small values of eccentricity is that these small eccentricity values are well outside the range of the data upon which the "old" relationship was developed. However, when used within its intended range of eccentricities and tubesheet bore displacement, the "old" method provides valid and conservative results. The "new" method of calculating the reduction in T/TS contact pressure is linear and directly accommodates small calculated values of eccentricity. It is also clear from the results in Table RAI4-7 that the results from the old method when used in its supported eccentricity range are highly conservative compared to the "new" method.

[a,c,e]

Figure RAI4-11
Original Figure RAI4-2 Discussed at the August 17, 2009 Meeting

4.2 Use of Both "Old" and "New" Fit

When establishing whether contact pressure increases when going from normal operating to steam line break conditions, how can a valid and conservative comparison be made if the normal operating case is based on the original delta contact pressure versus eccentricity curve and the SLB case is based on the new curve?

Response:

It is important to note than the new analysis method is only used for the SLB condition for the Model D5 steam generators. Comparison of contact pressures between the normal operating condition and the SLB condition is made for the Model F steam generators in the H* fleet in WCAP-17071-P on a consistent basis.

It is Westinghouse's engineering judgment that the old methodology provides an accurate determination of contact pressures during normal operating conditions and postulated accident conditions (FLB and SLB) when peak temperatures range between [ ]^{a,c,e} °F and eccentricities are between [ ]^{a,c,e} inch and [ ]^{a,c,e} inch and D_{max} and D_{min} are within [ ]^{a,c,e} % of each other.

Application of the new method to calculate eccentricities and values of D_{max} and D_{min} that fall outside the above noted range provides conservative results because the plane strain model upon which it based over-estimates the stiffness of the tube and tubesheet structure leading to lower contact pressure results as a function of eccentricity. The new method also excluded the effect of temperature and therefore, conservatively bounds the lower temperatures of the Model D5 SLB transient. The T/TS contact pressure results during SLB are still expected to bound the T/TS contact pressure results during NOP because, even though the tube bore eccentricity during SLB is generally greater than that during NOP, the overall growth of the tube bore during NOP is greater than that during SLB. Larger magnitudes of tube bore growth are directly related to decreasing tube-tubesheet contact pressure regardless of the value of calculated tube bore eccentricity.

It is appropriate to compare the Model D5 SLB contact pressure results from the "new" method to the Model D5 NOP results from the "old" method because each condition uses the appropriate fit to conservatively determine the reduction in T/TS contact pressure due to tube bore eccentricity and tube bore growth.

The sole purpose of the new methodology was to develop a more accurate way of calculating contact pressures during a postulated SLB for the Model D5 steam generators. The comparison provided in Figure 6-83 of WCAP-17072-P remains a valid comparison.

5.0 Part A (Original RAI#4)

Reference 1, Page 6-69: In Section 6.2.5.3, it is concluded that the tube outside diameter and the tubesheet tube bore inside diameter always maintain contact in the predicted range of tubesheet displacements. However, for tubes with through-wall cracks at the H* distance, there may be little or no net pressure acting on the tube for some distance above H*. In Tables 6-18 and 6-19, the fourth increment in the step that occurs two steps prior to the last step suggests that there may be no contact between the tube and tubesheet, over a portion of the circumference, for a distance above H*. Is the conclusion in 6.2.5.3 valid for the entire H* distance, given the possibility that the tubes may contain through-wall cracks at that location?

The following response to RAI#4 was included in Reference 11. The same response is included here to complete the record of information provided in regard to RAI#4 of References 5, 6 and 7.

Response:

The conclusions reached in Section 6.2.5.3 of WCAP-17071-P are valid for the entire H* distance because of the following considerations:

1. The primary source of contact pressure between the tube and the tubesheet is differential thermal expansion between the tubes and the tubesheet. The analysis in Section 6.2.5.3 specifically excludes the effect of thermal expansion of the tube from the analysis. The tubesheet is assumed to deform due to the combination of pressure and thermal loads which produces the tube bore ovalization and leads to the displacements applied in this model. Only the residual effects from installation are considered for the tube in steps 1 through 5. The tube internal pressure applied in these steps only simulates the hydraulic expansion pressure to establish the initial conditions for the following step. The conditions assumed for this study are not possible during any operating condition in the steam generator but are conservative relative to actual SG conditions. (Note: Residual contact pressure is not used in the calculation of H* values in Section 6. The residual effects of installation are included in the results of Section 6.2.5.3 so that the sensitivity of a strain hardened tube to tubesheet tube bore deformation can be studied.)

2. Step 5 on Tables 6-18 and 6-19 is not representative of any condition in the steam generator because it assumes that the tubesheet is at operating temperature with an applied primary-to-secondary pressure differential while the tubes remain at room temperature and are not pressurized. That is why Steps 1 through 5 are described as "initializing" steps in the process. It is physically impossible for these conditions to occur simultaneously in the same steam generator.

3. Because no pressure loading is applied to the tube in Step 5 of the analysis discussed in section 6.2.5, the results presented in Tables 6-18 and 6-19 are applicable regardless of whether, or not, a through-wall crack exists at the H* location. The more representative case is Step 6 shown on Tables 6-18 and 6-19 in which tube internal pressure is included. For that case, the potential point of zero contact pressure is at an applied displacement a factor of 5 greater than for Step 5, and far in excess of what is reasonably predicted for the actual tubesheet deformation. The factor of 5 difference in required displacement to cause the contact pressure to reduce to zero more than adequately covers the postulated potential local reduction in crevice pressure due to a circumferential separation at the location of H*. Recall also, that no thermal expansion of the tube is considered in this analysis.

It is also noted that tables 6-18 and 6-19 are the results of a sensitivity study that is not intended to represent the integrated calculation for H*. The integrated H* analysis is a complex process that combines the effects of several types of loading and deformation into an integrated estimate of the tube-to-tubesheet contact pressure. Therefore, it is not appropriate to consider a sensitivity study out of the context of the greater analysis. The integrated analysis presented in the complete Section 6 shows that for the combined case of the thermal effects, pressure effects, and tubesheet displacement there is tube-to-tubesheet contact pressure throughout the tubesheet.

It is acknowledged that the cut end of a tube is radially less stiff than a tube that is radially loaded at a point away from the tube end, and that the presumption of a tube sever at the H* distance may represent the case of a tube end. The decreased tube-end stiffness is referred to as "compliance." In other words, a tube that is loaded at the cut end provides less resistance to the load than a tube with equal load applied a distance removed from the tube-end. Thus, conceptually, a local "end effect" could be expected to occur due to the increased compliance of the tube-end.

The calculation process for H* shown in Figure 1-1 of the H* WCAP reports and discussed in several places in the report notes that an adjustment is made to the initial prediction of H* to account for the distributed crevice pressure referenced to the predicted H* position. Thus, the greatest crevice pressure is always located at the final value of H*. Increased tube compliance cannot result in a higher local crevice pressure than is already included in the analysis because, at the point of sever, the primary side pressure is the crevice pressure.

It may be postulated that the increased tube compliance results in reduced contact pressure because the net differential pressure across the tube wall is zero. At the tube-end, the current analysis already includes a zero differential pressure due to the adjustment process for distributed crevice pressure. Therefore, the net reduction in contact pressure would be limited to the axial length of the local effect and would further depend on the slope of the decrease in crevice pressure.

For the Model F and Model D5 SGs, the bounding value of isolation distance above the tube end is 0.6 inch based on classical solutions for the design of pressure vessels (Timoshenko).

The isolation distance is the generically applicable minimum separation distance from an applied load to a point of interest in order to safely assume that the load is in the far field relative to the point of interest. Specific structures and load cases may have different isolation distances but the classical result by Timoshenko for a pressure vessel will conservatively bound any specific cases. For this length, the slope of the contact pressure curve would have to decrease by a factor of at least [ ]^{a,c,e} before the value of H* is affected by more than [ ]^{a,c,e} inch. If the tube is conservatively modeled as a center-loaded beam on an elastic foundation compared to an end-loaded beam on an elastic foundation, the resulting worst case change in structural compliance and the resulting contact pressure slope could be a factor of up to 2. Alternatively, similar analyses for the cross sections of curved beams suggest that the change in compliance of the structure could be as high as a factor of 6. Neither case approaches the factor of [ ]^{a,c,e} required based on classical pressure vessel analysis to impact the value of H*; therefore, no additional adjustments to H* are necessary to address the potential end effects.

6.0 Summary of the Response to RAI #4

A summary of the response to the original RAI# 4 and additional questions related to RAI 4 are provided below:

1. No additional adjustment to the value for H* is necessary to address the potential for end effects. This is because the greatest crevice pressure is always located at the final value of H*. At the H* distance, the current analysis already includes a zero pressure differential due to the adjustment process for the distributed crevice pressure. Therefore, the net reduction in contact pressure would be limited to the axial length of the local effect and would further depend on the slope of the decrease in crevice pressure. It is judged that the slope of the contact pressure curve would not decrease at a rate such that the value of H* would be affected.

2. Tube bore dilation is a more significant factor in determining tube-to-tubesheet contact pressure at higher temperatures and the effect of eccentricity on contact pressure is reduced at higher temperatures. The methodology for addressing the effect of eccentricity on contact pressure discussed in Reference 6-15 and utilized in WCAP-17071-P, WCAP-17072-P, WCAP-17091-P and WCAP-17092-P reflects this fact and, therefore, it provides acceptably accurate contact pressure results at higher temperatures (i.e., for all conditions except the "colder" SLB condition). This includes NOP, SLB (higher temperature, > 400°F, and FLB, where appropriate).

3. The results of using the fit described in Reference 6-15 match the expected trend from a best case finite element model for the NOP and SLB conditions for the Model F SGs and NOP conditions for the Model D5 SG.

4. The ΔDs from the 3D FEA model are significantly less than the corresponding ΔDs from the unit cell model from the unloaded to the fully loaded condition (i.e.,

from step 0 to step 9) for both NOP and SLB conditions. This leads to the conclusion that the unit cell model displacement results and contact pressure predictions conservatively represent the reference 3D FEA model results.

5. The eccentricities from the unit cell model are generally comparable to those from the 3D FEA model. A more exact comparison is difficult based on the available data; however, it is clear that the actual range of eccentricities from the 3D FEA model was adequately addressed by the unit cell model.

6. Based on items 4) and 5) which demonstrate the acceptability of the use of the unit cell model for benchmarking the 3-D FEA model, the method for calculating the reduction in contact pressure defined by the unit cell model, when adjusted for temperature effects, shows that SLB contact pressure is increased relative to normal operating conditions for the Model D5 steam generators.

7. It has also been shown when comparing contact pressures for NOP conditions for the unit cell to contact pressures for SLB for the unit cell for the Model F SG (higher temperature SLB conditions), that contact pressure increases during a postulated SLB.

8. Given that the two structural models provide similar eccentricities, the unit cell model shows that for these eccentricities, positive contact pressure exists between the tubes and the tubesheet for the entire range of displacements considered.

Based on the above, it is concluded that the NOP contact pressures that define H* in the Model F and Model D5 SG are conservative and that a more realistic model of contact pressure reduction as a function of tube bore deformation (including both dilation and eccentricity) would predict positive contact pressure around the entire circumference of the tube and an increase in tube to tubesheet contact pressure at SLB conditions compared to NOP conditions.

The conclusions reached in the response to RAI#4 apply equally for the Model 44F and Model 51F SGs.

ATTACHMENT 16

Westinghouse Letter LTR-SGMP-10-34 Rev. 2, "An Assessment of the Impact of Revised Normal Operating Conditions on the Catawba Unit 2 H* Calculations" (Non-Proprietary)

Westinghouse

To: Doug Warren
cc: H.O. Lagally
D.A Testa
C.D. Cassino
C.L. Hammer

From: Steam Generator Management Programs
Ext: 724-722-5584
Fax: 724-722-5889

Date: April 27, 2010

Our ref: LTR-SGMP-10-34 Rev. 2

Subject: **An Assessment of the Impact of Revised Normal Operating Conditions on the Catawba Unit 2 H* Calculations**

References:

1. WCAP-17072-P, "H*: Alternate Repair Criteria for the Tubesheet Expansion Region in Steam Generators with Hydraulically Expanded Tubes (Model D5)," May 2009.
2. Duke Energy Letter; "Inputs for Verification that the H* Technical Justification Report, WCAP-17072-P, Bounds the Current Catawba Nuclear Station's Design Parameters," March 24, 2010.
3. LTR-SGMP-09-100 P-Attachment, "Responses to NRC Request for Additional Information on H*; Model F and Model D5 Steam Generators," August 14, 2009.

This letter has been revised to remove information that is considered Westinghouse proprietary.

The operating conditions identified in Reference 1 have been used to calculate the H* lengths and the primary-to-secondary leakage factors for the Catawba Unit 2 steam generators (SGs). At the request of Duke Energy, an evaluation has been completed to determine whether or not the H* lengths and leakage factors calculated at the normal operating conditions (NOP) in References 1 and 3 (leakage factors only) remain bounding at the operating conditions identified in Reference 2. This correspondence provides the results of the requested evaluation. The key operating temperatures and pressures that are considered for this evaluation for the revised conditions are provided in Table 1 of this correspondence.

From a tube pullout capability perspective, as discussed in Reference 1, the limiting H* length calculated for the Catawba Unit 2 steam generators is based on the low T_{avg} normal operating (NOP) condition loadings (i.e., 3 times NOP pressure differential) for the limiting Model D5 steam generators in the H* fleet, which are at Byron and Braidwood Unit 2. The pressure differential that occurs across the tubesheet during NOP conditions in Reference 2 (1280 psid) is bounded by the limiting plant condition (by greater than 100 psid). Based on this fact, coupled with a minimal change in SG inlet and outlet temperatures of less than 3°F at the operating conditions in Reference 2 (which would result in a negligible change in temperature displacements in the tubesheet in the conservative direction as the hot leg temperature condition is limiting), it is concluded that no changes in the calculated H* lengths in Reference 1 are required for Catawba Unit 2.

From a leakage perspective, plant-specific normal operating conditions were used as initial conditions to calculate the resultant leakage factors. As explained in Reference 1, the resultant leakage factors are the result of the product of the pressure differential and viscosity subfactors that are developed using the Darcy Formula for flow through a porous medium. The limiting transient for determining the leakage factor for inclusion in the Catawba Unit 2 Technical Specifications is the postulated feedwater line break event and the greatest temperature rise in the tubes occurs on the cold leg side of the Model D5 SG. The initial SG cold leg temperature for normal operating conditions in Reference 2 (558 °F) is significantly greater than the SG outlet temperature included in Reference 1 (by approximately 15 °F). This results in an increase in dynamic viscosity subfactor during the postulated feedwater line break event. When coupled with the increase in pressure differential ratio subfactor that occurs during the feedwater line break (FLB) event due to the decreased pressure differential across the tubesheet during normal operating conditions in Reference 2, the product of the resulting leakage subfactors increases from 2.65 to 3.27.

Based on the above, it is concluded from a structural perspective that the operation of Catawba Unit 2 at the Reference 2 conditions is bounded by the results included in Reference 1 and no changes to the H* lengths are necessary. However, from a tube leakage perspective, the feedwater line break leakage factor reported in Reference 3 needs to be revised upwards from 2.65 to 3.27.

Please transmit this information to Dan Mayes of Duke Energy.

Author:

Electronically Approved

G.W. Whiteman
Principal Engineer
Regulatory Compliance and Plant Licensing

Verifier:

Electronically Approved

H.O. Lagally
Fellow Engineer
Steam Generator Management Programs

Manager:

Electronically Approved

D. A. Testa
Manager
Steam Generator Management Programs

Table 1 Key Operating Parameters – Catawba Unit 2 Normal Operating Conditions	
Analysis Parameters	Revised Operating Conditions (note 1)
	Catawba Unit 2 (Reference 2)
Primary Side Pressure (psia)	2250
Secondary Side Pressure (psia)	970
Primary-to-Secondary Pressure Differential (psid)	1280
Primary Fluid SG Inlet Temperature (°F)	616.7
Primary Fluid SG Outlet Temperature (°F)	558

Notes:
1. Values apply for 0% plugging because this results in the highest steam pressure (see Reference 2) and thus the highest leakage factor (see Reference 1).

ATTACHMENT 17

Summary of Regulatory Commitments

Summary of Regulatory Commitments

This table identifies commitments made in this amendment request. Any other actions discussed in this submittal represent intended or planned actions. They are described to the NRC for the NRC's information and are not regulatory commitments.

Commitment	Committed Date or Outage	One-Time Action (Yes/No)	Programmatic Action (Yes/No)
Catawba commits to monitor for tube slippage as part of the SG tube inspection program. Applicable to Catawba Unit 2 End of Cycle 17 Refueling Outage and subsequent Cycle 18 operation.	During scheduled inspection required by TS 5.5.9, "Steam Generator (SG) Program" for Catawba Unit 2 End of Cycle 17 Refueling Outage and subsequent Cycle 18 operation.	Yes	No
Catawba commits to perform a one-time verification of the tube expansion to locate any significant deviations in the distance from the top of the tubesheet to the bottom of the expansion transition (BET). If any deviations are found, the condition will be entered into the corrective action program and dispositioned. Additionally, Catawba commits to notify the NRC of significant deviations. Applicable to Catawba Unit 2 End of Cycle 17 Refueling Outage.	Required to be completed prior to entering Mode 4 following the SG tube inspection performed during the Catawba Unit 2 End of Cycle 17 Refueling Outage.	Yes	No
For the Condition Monitoring (CM) assessment, the component of	During scheduled inspection required by TS 5.5.9, "Steam Generator (SG) Program" for Catawba Unit 2 End of Cycle	Yes	No

operational leakage from the prior cycle from below the H* distance will be multiplied by a factor of 3.27 and added to the total accident leakage from any other source and compared to the allowable accident induced leakage limit. For the Operational Assessment (OA), the difference between the allowable accident induced leakage and the accident induced leakage from sources other than the tubesheet expansion region will be divided by 3.27 and compared to the observed operational leakage. An administrative operational leakage limit will be established to not exceed the calculated value. Applicable to Catawba Unit 2 End of Cycle 17 Refueling Outage and subsequent Cycle 18 operation.	17 Refueling Outage and subsequent Cycle 18 operation.		